

Preparation and ferroelectric properties of Bi-modified lead zirconate titanate thin film

K. B. LEE, S. K. CHO*

Department of Physics, and *Department of Chemistry, Sangji University, Wonju, Kangwondo 220-702, Korea
E-mail: skcho@chiak.sangji.ac.kr

We have studied the structural and electrical properties of bismuth-modified lead zirconate titanate thin films. Specimens with various Bi contents, $(\text{Pb}_{1-3/2x}\text{Bi}_x)(\text{Zr}_{0.52}\text{Ti}_{0.48})\text{O}_3$ (PBZT) thin films, were prepared on a Pt-coated Si wafer by the sol–gel method. Ferroelectricity confirmed by the measurement of dielectric constant and P–E hysteresis loop was found for specimens below $x = 0.25$, in which the values of both dielectric constant and remanent polarization were decreased with increasing Bi contents. The behaviors of the electrical properties with Bi content corresponded to the structural changes by increasing non-ferroelectric cubic phase with increasing Bi contents, which was thought to be due to the vacancies in Pb-sites created by the substitution of Bi into Pb. © 1998 Kluwer Academic Publishers

1. Introduction

Ferroelectric thin films have been intensively studied over the past years as candidates for use of ultra-large-scale-integration (ULSI) dynamic random access memories (DRAM) and non-volatile ferroelectric random access memories (NVFRAM). Among them, ferroelectric $\text{Pb}(\text{Zr}, \text{Ti})\text{O}_3$ (PZT) thin film is one of the promising NVFRAM materials [1], as well as $\text{SrBi}_2\text{Ta}_2\text{O}_9$ thin film [2]. A variety of PZT-based materials compatible for the specific applications such as electro-optic sensors [3] and electromechanical systems [4] as well as memory dielectrics have been developed, via changes in the chemical synthesis and processing method and different compositional modifications. The aliovalent substitution of Pb by La [5] in PZT (PLZT) thin films have been intensively studied for those specific applications, and their structural and electrical properties are well-known as compared with the other PZT-based thin films.

In this paper, we used bismuth (Bi) as a new modifier for PZT thin film because any information about PBZT thin films has not yet been reported. We prepared the PBZT thin films with various Bi contents and a Zr/Ti ratio of 52/48, that is, $(\text{Pb}_{1-3/2x}\text{Bi}_x)(\text{Zr}_{0.52}\text{Ti}_{0.48})\text{O}_3$, by the sol–gel method and investigated the structural and electrical properties of PBZT thin films with respect to Bi contents.

2. Experimental procedure

The sol–gel method used in this experiment is shown as a flow chart in Fig. 1. The starting materials were lead acetate trihydrate, titanium isopropoxide, zirconium *n*-propoxide, and bismuth nitrate. Acetic acid and 2-methoxyethanol were selected as solvents. The mixture of titanium isopropoxide and zirconium *n*-propoxide

was diluted with 2-methoxyethanol. Before lead acetate trihydrate was added, bismuth nitrate that was initially dissolved in glacial acetic acid was added to this mixture. To compensate for Pb loss during firing, 10 mol % excess Pb, as compared to the stoichiometry ABO_3 , was incorporated in this procedure. A clear and viscous solution was obtained by boiling sol to 190 °C, at which low boiling reaction products such as isopropanol, *n*-propanol, acetic acid, and water were distilled off. The coating solutions were finally used by diluting with 2-methoxyethanol to adjust the concentration to 0.5 M.

PBZT thin film was deposited onto a substrate by spin-casting a coating sol at 3000 rpm for 1 min. The substrate consisted of a multi-layer of Pt/Ti/SiO₂/Si, where the SiO₂ layer of about 200 nm thickness was made by thermal oxidation of the Si wafer, the Ti layer of about 100 nm thickness by d.c. magnetron sputtering, and the Pt layer of about 500 nm thickness by r.f. magnetron sputtering. Wet PBZT film was dried in air at 80 °C by using a infrared lamp and put on a hot plate at 200 °C for 5 min. The post-annealing process was done at 650 °C for 10 min in a pre-heated tubular furnace. After these coating and heat-treatment processes were repeated up to four times, PBZT films of about 400 nm thickness, which was measured by scanning electron microscope (SEM), as shown in Fig. 2. The crystal structure was investigated by X-ray diffraction (XRD) using CuK_α radiation.

To measure the electrical properties of PBZT thin films, a Pt–upper electrode with 0.3 mm diameter was sputtered on the PBZT layer by r.f. magnetron sputtering using shadow mask. Both dielectric constant and dissipation factor were measured using an LCZ meter (NF 2232). The P–E hysteresis curves were measured using a standard Ferroelectric Tester (RT66A,

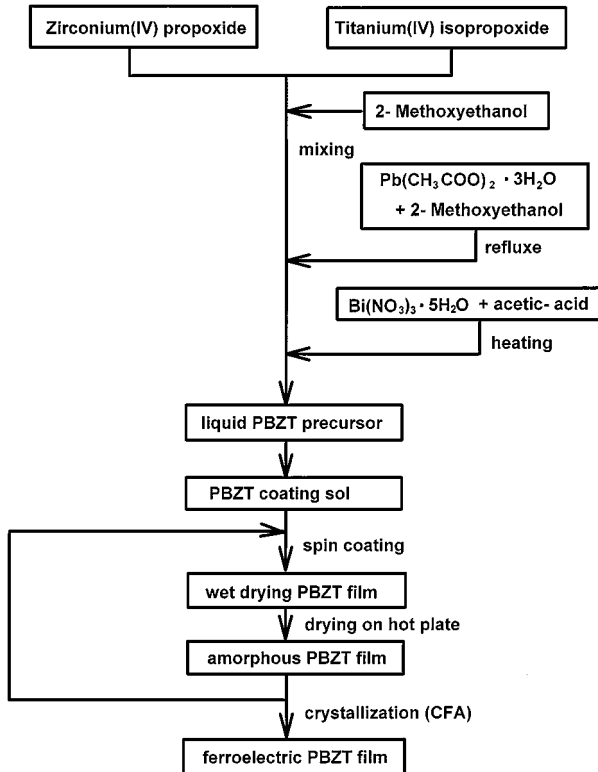


Figure 1 Schematic of the sol-gel method for preparing $(\text{Pb}_{1-3/2x} \text{Bi}_x) (\text{Zr}_{0.52} \text{Ti}_{0.48})\text{O}_3$ thin films.

Radiant Technologies) and I-V curves using Picoammeter/Source (Keithley 417). All data acquisition and processing of these electrical measurements were provided by an IBM PC/AT.

3. Results and discussion

We found some fundamental electrical properties of PBZT thin films with the Bi contents of 0.0 to 0.30,

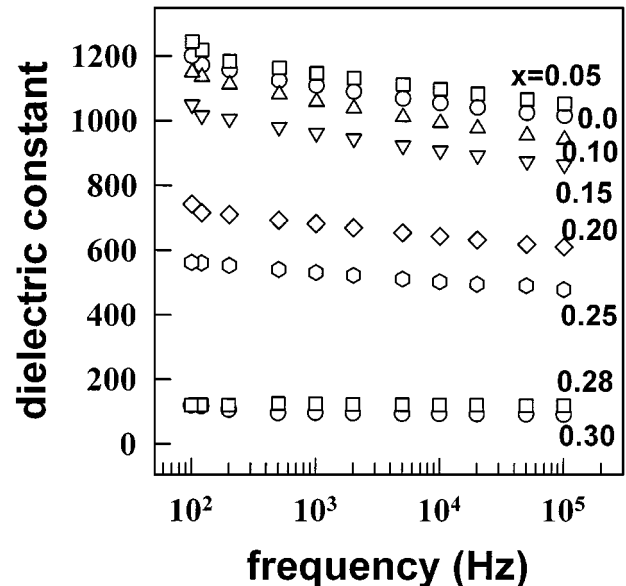


Figure 3 Frequency dependence of dielectric constant for PBZT thin films.

which were annealed at 650 °C during 10 min. Fig. 3 shows the frequency dependence of the dielectric constant for PBZT thin film capacitors with different Bi contents, where an oscillating voltage is 0.05 V. The frequency dependence of the dielectric constant for all specimens is very similar in that the dielectric constant is slightly decreasing with increasing frequency. The relation of the magnitude of the dielectric constant at 100 kHz and Bi contents in PBZT thin films is plotted in Fig. 4. The maximum value of the dielectric constant is 1050 for PBZT thin film with Bi contents of $x = 0.05$, which is larger than that for PZT thin film without Bi, and the dielectric constant decreases linearly from this maximum value to 450 for PBZT thin film with Bi contents of $x = 0.25$. As shown in Fig. 4, the dissipation

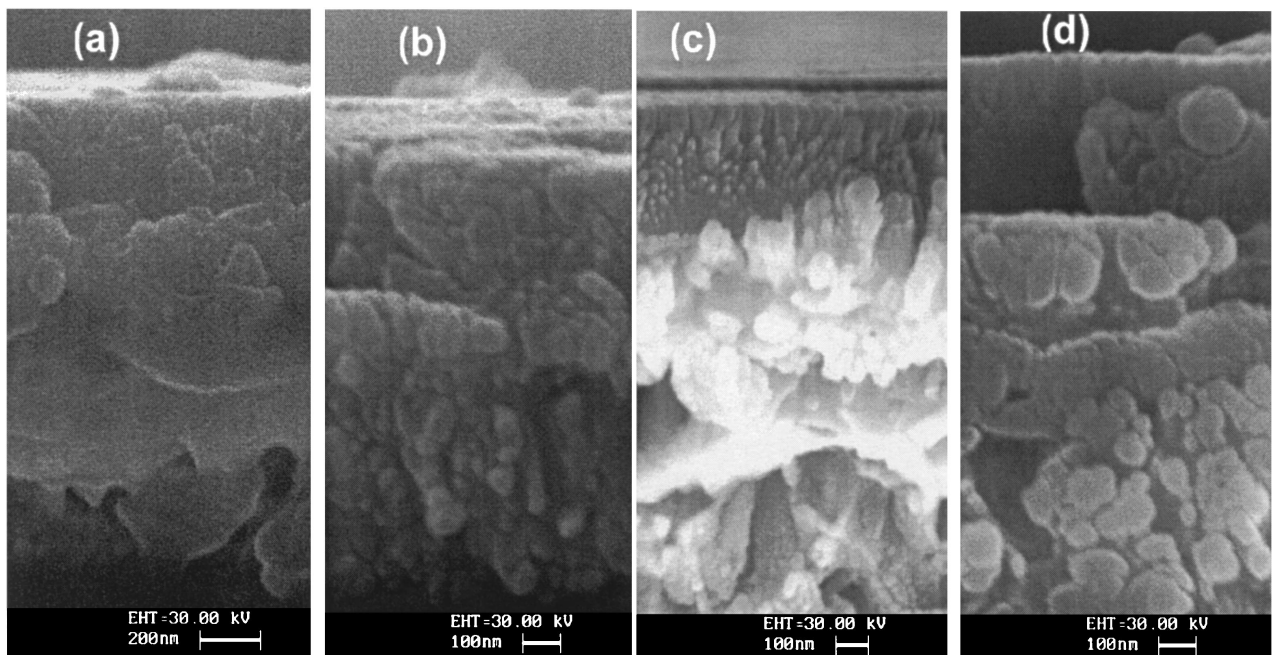


Figure 2 Typical cross-sectional SEM images of PBZT thin films with (a) $x = 0.0$; (b) $x = 0.05$; (c) $x = 0.15$; and (d) $x = 0.25$, deposited on Pt/Ti/SiO₂/Si wafers.

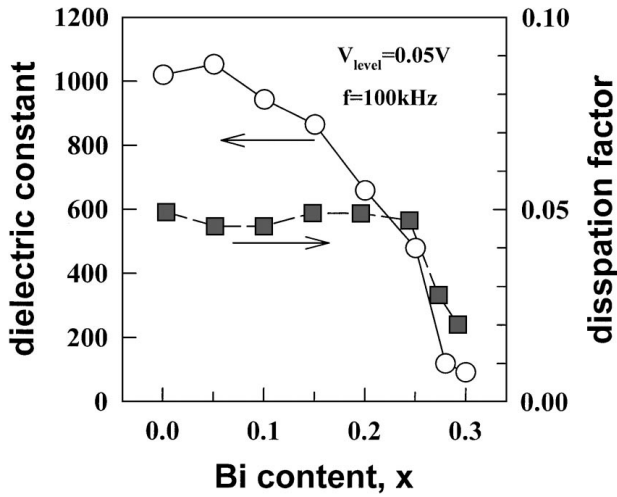


Figure 4 Plot of dielectric constant and dissipation factor as a function of Bi content in PBZT thin films.

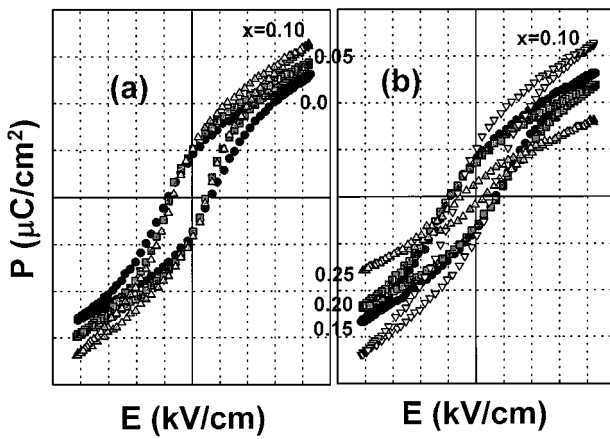


Figure 5 P-E hysteresis curves of ferroelectric PBZT thin films with Bi content of (a) $x = 0.0, 0.05$, and 0.10 ; and (b) $x = 0.10, 0.15, 0.20$, and 0.25 .

factor is about 0.05 for ferroelectric specimens and is about 0.02 for paraelectric specimens.

Ferroelectricity of PBZT thin films could be confirmed by the measurement of the P-E hysteresis curves, as shown in Fig. 5a and b. The maximum polarization increases as Bi contents are 0.0 to 0.10 and subsequently decreases as Bi contents are 0.10 to 0.25. The hysteresis loop for PBZT thin films with Bi contents of 0.28 and 0.30 could not be found. In Fig. 6, P-E hysteresis characteristics such as remanent polarization, P_r , and coercive field, E_c , which were estimated from Fig. 5a and b, were shown as a function of Bi contents. The values of P_r and E_c for ferroelectric PBZT thin films are in the range of 3.2 to $11.4 \mu\text{C}/\text{cm}^2$ and 38 to $64 \text{ kV}/\text{cm}$, respectively. It is very interesting that the behaviors of P_r and E_c with Bi contents are nearly the same as those of the dielectric constant and dissipation factor in Fig. 4, respectively. Although the similarity of the behavior of dielectric characteristics and that of hysteresis characteristics is unfavorable to the device application such as DRAM and FRAM, the ferroelectric PBZT thin films prepared in our experiment are worthwhile for devices using their ferroelectric properties.

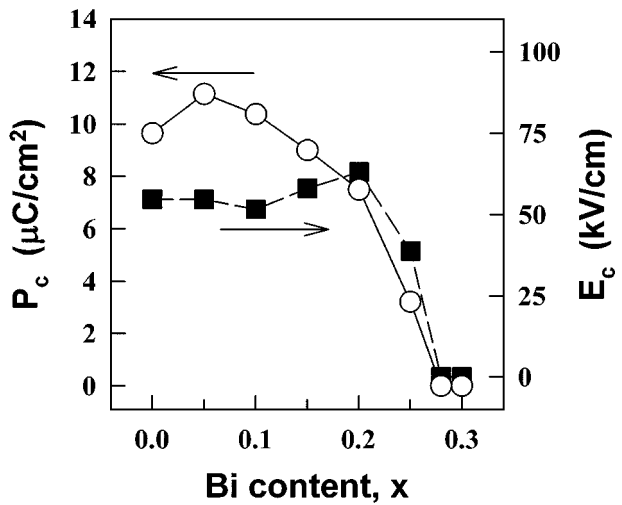


Figure 6 Plot of remanent polarization and coercive field as a function of Bi content in ferroelectric PBZT thin films.

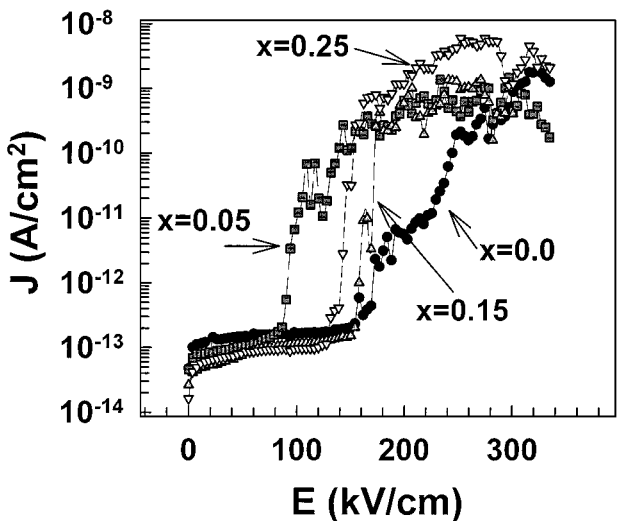


Figure 7 Typical current-voltage characteristics of ferroelectric PBZT thin films with $x = 0.0, 0.05, 0.15$, and 0.25 .

Fig. 7 shows the typical time-zero current-voltage characteristics [6] for the ferroelectric PBZT thin film capacitors with Bi contents of $x = 0, 0.5, 0.15$, and 0.25 . Any special tendency was not found between the current-voltage characteristic curves and Bi contents in Fig. 7. This means the current-voltage characteristics depend not only on microstructure and composition of the film but also on the interfacial reaction between the electrode and the film. The low current region is extended to more than 5 V (or $125 \text{ kV}/\text{cm}$ in electric field unit), which is larger than the maximum operational voltage, 3.3 V , for 256 M DRAM . [7] The leakage current densities at 3 V ($75 \text{ kV}/\text{cm}$ in electric field unit) are in the range of 1.7×10^{-7} to $3.2 \times 10^{-7} \text{ Acm}^{-2}$ for various Bi contents, which are enough low for the practical applications.

To elucidate the electrical properties with respect to Bi content in terms of the structural changes by Bi-modification, XRD curves were investigated for post-annealed specimens at 650°C for 10 min, as shown in Fig. 8. Bi contents, x , in each PBZT thin films were

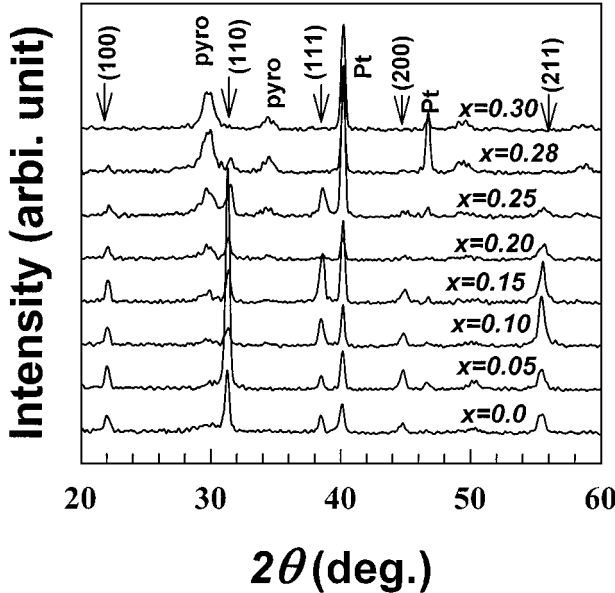


Figure 8 XRD patterns of PBZT thin films annealed at 650 °C for 10 min.

denoted on each curve. It was found that the perovskite phases are found for specimens with a Bi content up to $x = 0.28$, which implies that the maximum Bi content, x , to get the ferroelectric perovskite phase is about 0.28, which is larger than that for La in PLZT [5]. It is also found that all of PBZT thin films are randomly oriented with a preferential orientation of (110), except the one with $x = 0.05$, having a pronounced and sharp (110) peak. The intensity ratio of the pyrochlore phase to the perovskite phase is increased, and the intensity of (110) peak is decreased with increasing x . Because the dielectric constant is inversely proportional to the intensity ratio of the pyrochlore phase to the perovskite phase, and it also has a larger value for the highly oriented ferroelectric thin film than for the randomly oriented one, the behavior of the dielectric constant with Bi contents is consistent with these XRD results.

To determine the phase transition temperature with respect to Bi content in PBZT thin film, differential thermal analysis (DTA) and thermogravimetry (TG) measurements were carried out simultaneously in the temperature range of 100~700 °C at a heating-up scan rate of 10 °C min⁻¹. Dried gel made by hydrolysis of PBZT coating sol at 200 °C was used in DTA measurement. In the DTA and TG curves shown in Fig. 9, the broad exothermic valleys around 280 °C associated with some relaxation mechanism in the amorphous structure, and the shallow endothermic peaks around 440 °C and the second exothermic valleys around 480 °C were known to correspond with nucleation and crystallization of the metastable non-ferroelectric pyrochlore phase, respectively [8]. Other broad, small endothermic peaks that were related to the transition from the pyrochlore phase to the stable ferroelectric perovskite one [8] appeared around 630 °C for all PBZT thin films. These peaks shift slightly to lower temperature as Bi contents increase. Hence, the increase of the pyrochlore phase with the increase of Bi content was not associated with the effect that resulted in the difference between the annealing

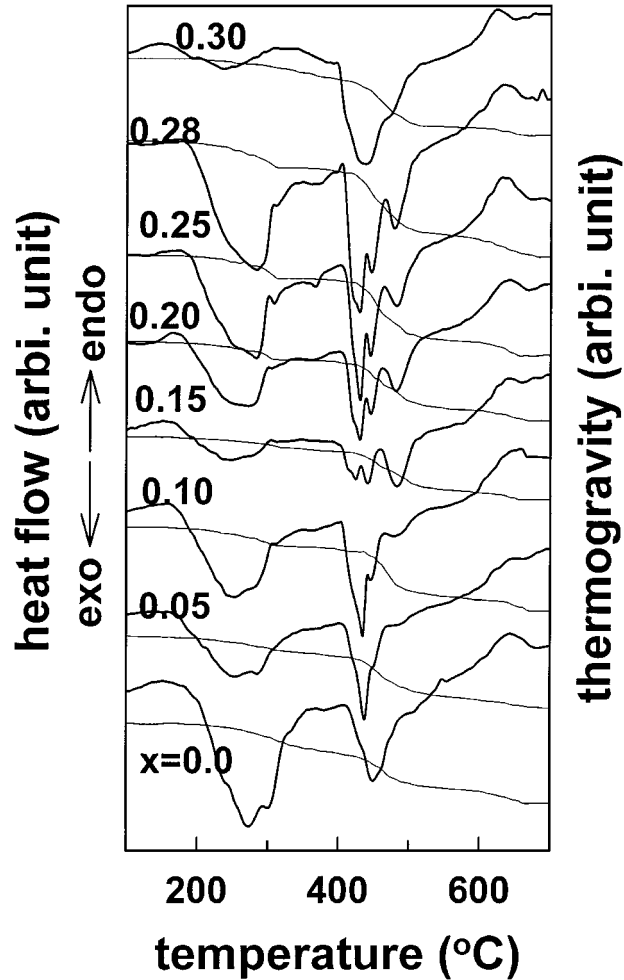


Figure 9 DTA and TG curves of PBZT dried gels. Bi content, x , is denoted on each curve.

temperature of 650 °C and the crystallization temperature to obtain ferroelectricity for given Bi content.

Ferroelectricity of a tetragonal perovskite ABO_3 is due to the permanent dipole produced by the up-and-down displacement of the B^{4+} ions along the c-axis with respect to the other ions such as O^{2-} . The aliovalent substitution of Pb^{2+} by Bi^{3+} creates vacancies on the A-site in PZT. The incorporation of Bi and vacancy is believed to break the long-range interaction between ferroelectrically active octahedral B-site cations. Breaking the long-range interaction is thought to give rise to the decrease of grain size with the increase of Bi content, which corresponds to the decrease of the (110) peak with the increase of Bi content. The increase of the ratio of the pyrochlore phase to the perovskite one with the increase of Bi content, as seen in Fig. 8, can be also explained as following. Vacancies on A-site in PZT can give rise to the other microstructural changes. These reduce the dipole moment due to the weaker interaction between the A ion and B ion or the oxygen ion. Hence, the transformation from the tetragonal structure to the non-ferroelectric cubic one increases as Bi content increases. The exceptional XRD results in Fig. 8 for PBZT thin film with Bi content of $x = 0.05$ imply that this specimen has densely packed and highly oriented crystallinity with large grains. Though we cannot explain clearly about the fundamental origins of

these results, we presume that they are resulted from the unexpected or extrinsic problems on preparing PBZT precursors such as the mismatch between the intended ratio and the real batch ratio of $(\text{Pb} + \text{Bi})/(\text{Zr} + \text{Ti})$.

4. Conclusion

Bi-doped ferroelectric lead zirconate titanate $(\text{Pb}_{1-3/2x} \text{Bi}_x)(\text{Zr}_{0.52} \text{Ti}_{0.48})\text{O}_3$ thin films were prepared on Pt-coated Si wafers by means of the sol-gel method. The maximum Bi content having ferroelectric perovskite phase was about $x = 0.28$, which was larger than that of La-modified PZT thin films. The electrical properties such as dielectric constant and remanent polarization is consistent with the structural properties in ferroelectric Bi-modified PZT thin film, which implies that the negatively charged vacancies in the Pb-site created by modifying of Bi play an important role in the structural and electrical properties of ferroelectric Bi-modified PZT thin films.

References

1. R. E. JONES, JR. and S. B. DESU, *MRS Bulletin* **21** (1996) 55.
2. J. F. SCOTT, F. M. ROSS, C. A. PAZ DE ARAUJO, M. C. SCOTT and M. HUFFMAN, *ibid.* **21** (1996) 33.
3. D. DIMOS, W. L. WARREN and B. A. TUTTLE, *Mat. Res. Soc. Symp. Proc.* **310** (1993) 87.
4. D. L. POLLAK and L. F. FRANCIS, *MRS Bulletin* **21** (1996) 59.
5. G. TEOOWEE, E. L. QUACKENBUSH, C. D. BAERTLEIN, J. M. BOULTON, E. A. KNEER and D. R. UHLMANN, *Mat. Res. Soc. Symp. Proc.* **361** (1995) 433.
6. C. SUDHAMA, A. C. CAMPBELL, P. D. MANIAR, R. E. JONES, R. MOAZZAMI, C. J. MOGAB and J. C. LEE, *J. Appl. Phys.* **75** (1994) 1014.
7. B. E. GNADE, S. R. SUMMERFELT and D. CRENSHAW, "Science and Technology of Electroceramic Thin Films" (NATO ASI Series, 1994) p. 373.
8. H. HU, C. J. PENG and S. B. KRUPANIDHI, *Thin Solid Films* **223** (1993) 327.

*Received 29 October 1996
and accepted 1 June 1998*